Acoustically evoked K-complexes are sufficient to boost verbal memory consolidation during sleep

Sven Leach[a], Elena Krugliakova[a], Georgia Sousouri[a,*], Sophia Snipes[a,*], Jelena Skorucak[a,*], Selina Schühle[a,*], Manuel Müller[a,*], Maria Laura Ferster[b,*], Giulia Da Poian[c,*], Walter Karlen[b,d], Reto Huber[a,e,**]

[a] Child Development Centre and Children's Research Centre, University Children's Hospital Zurich, University of Zurich, Zurich, Switzerland
[b] Mobile Health Systems Lab, Department of Health Sciences and Technology, Institute of Robotics and Intelligent Systems, ETH Zurich, Zurich, Switzerland
[c] Sensory-Motor Systems Lab, Department of Health Sciences and Technology, ETH Zurich, Zurich, Switzerland
[d] Institute of Biomedical Engineering, Faculty of Engineering, Computer Science and Psychology, Ulm University, Ulm, Germany
[e] Department of Child and Adolescent Psychiatry and Psychotherapy, Psychiatric Hospital, University of Zurich, Zurich, Switzerland

Abstract

The pivotal role of sleep in memory consolidation is widely acknowledged, yet which specific electrophysiological components drive this process remains a topic of intense debate. To unveil this process, a neuromodulation approach enabling the precise manipulation of specific oscillations is necessary. Here, we combined phase-targeted auditory stimulation (PTAS) during sleep in combination with high-density electroencephalography (hd-EEG) to specifically evoke K-complexes (KCs), a prominent oscillation during non-rapid-eye-movement (NREM) sleep. Over the course of two nights, one with PTAS, the other without, data from 14 young healthy adults were recorded. By targeting the down-phase of slow waves, auditory stimuli selectively evoked KCs. Strikingly, these evoked KCs were associated with improved verbal memory consolidation via enhanced cross-frequency coupling between slow waves and spindles in a right frontal region. This finding suggests that evoked KCs actively participate in the hippocampal-neocortical dialogue and thereby drive the consolidation of memories during sleep.

Keywords: sleep, memory, auditory stimulation, closed-loop, phase-targeted, K-complex, acoustically evoked, memory consolidation, declarative memory, verbal memory, causality, cross-frequency coupling, slow-wave-spindle coupling, high-density EEG

Introduction

Memory is a fundamental cornerstone of our daily cognitive experience, critical for human mental functioning and exerting a profound impact on our sense of self. An instrumental component in the formation of memories is consolidation, a process that involves the integration and stabilization of new information within pre-existing neuronal networks (Squire et al., 2015). Sleep plays an indispensable role in this process (Stickgold, 2005; Rasch and Born, 2013; Genzel et al., 2014; Klinzing et al., 2019). Particularly during non-rapid eye movement (NREM) sleep, neuronal networks that host memory representations are reorganized and synaptic weights between participating neurons are adjusted (Tononi and Cirelli, 2014; González-Rueda et al., 2018; Abel et al., 2013). High-amplitude slow waves (0.5 – 4 Hz) and sleep spindles (11 – 16 Hz), the two most prominent electrophysiological oscillations in the electroencephalogram (EEG) during NREM sleep (Steriade et al., 1993; Timofeev and Chauvette, 2017; Fernandez and Lüthi, 2020), are intimately connected to these memory consolidation processes (Latchoumane et al., 2017a; Helfrich et al., 2018; Hahn et al., 2020).

At the neuronal level, slow waves arise from the synchronized activity of extensive neuronal networks, which undergo rhythmic transitions between cortical up-states (neuronal firing) and down-states (neuronal silence; Steriade et al., 1993; Crunelli et al., 2012). Recent endeavors aimed at classifying slow waves according to their spatial and temporal features (Bernardi et al., 2018; Siclari et al., 2014; Navarrete et al., 2022). This has sparked discussions regarding their potentially distinct contributions to memory and other vital processes, such as immune functions (Zielinski and Krueger, 2011) or glymphatic clearance (Schreiner et al., 2019). To date, the precise contributions of slow oscillations (SOs; widespread, large-amplitude waves of cortico-thalamic origin; 0.5 – 1 Hz; Bernardi et al., 2018; Siclari et al., 2014; Navarrete et al., 2022) and delta waves (somewhat faster, 1 – 4 Hz, more focal slow waves of cortico-cortical origin; Bernardi et al., 2018; Siclari et al., 2014; Navarrete et al., 2022) on memory consolidation remain elusive.

Nonetheless, an increasing body of research suggests that the synchronization of sleep spindles with

[*] In reversed alphabetical order
[**] Corresponding author
[1] Email: leachsven+roleofkc@gmail.com (first author); reto.huber@kispi.uzh.com (corresponding author)

[2] Abbreviations: K-complex (KC), slow-wave activity (SWA), phase-targeted auditory stimulation (PTAS), slow oscillation (SO), high-density electroencephalography (hd-EEG), electromyography (EMG), electrocardiography (ecg), non-rapid eye movement (NREM), rapid eye movement (REM), inter-stimulus interval (ISI), false discovery rate (FDR), auditory evoked potential (AEP), event-related spectral potential (ERSP), inter-trial coherence (ITC), z-standardized modulation index (zMI), region of interest (ROI), American Academy of Sleep Medicine (AASM), power spectral density (PSD), finite impulse response (FIR), graphical user interface (GUI), mean (M), standard deviation (SD)

the up-phase of slow waves reflects a pivotal mechanism for memory consolidation (Staresina et al., 2015; Latchoumane et al., 2017b). This coupling potentially represents a privileged window of communication between the hippocampus and neocortex that is crucial for sleep-dependent memory consolidation (active systems consolidation concept; Diekelmann and Born, 2010; Rasch and Born, 2013; Lewis and Durrant, 2011; Klinzing et al., 2019; Cox et al., 2019).

An intriguing type of slow wave that frequently couples with sleep spindles during its up-phase (Stern, 2005; Loomis et al., 1935; Colrain, 2005; Halász, 2005) is known as the K-complex (KC; large-amplitude waves with broad fronto-central topographies; Bernardi et al., 2018; Dang-Vu et al., 2008; Genzel et al., 2014; Mölle et al., 2002; Siclari et al., 2014). KCs exhibit remarkable similarities to individual SOs while simultaneously displaying spectral characteristics within the delta frequency range (Amzica and Steriade, 1997). Despite being a defining feature of NREM sleep, the role of KCs in essential functions associated with sleep remains a subject of ongoing debate.

Animal studies have yielded compelling evidence endorsing the involvement of KCs in hippocampal-neocortical communication (Ego-Stengel and Wilson, 2010; Isomura et al., 2006; Sirota et al., 2003; Peyrache et al., 2011; Wierzynski et al., 2009). Despite their valuable contributions, these studies fall short of providing a conclusive answer regarding the direct influence of KCs on memory domains specific to humans, such as verbal memory.

In humans, the current evidence supporting the involvement of KCs in memory processes is primarily based on correlational studies without experimental manipulations (De Gennaro et al., 2017). While it is possible to reliably evoke KCs using salient auditory stimuli (e.g., a "knock" on the door, thus "K"-complex; Davis et al., 1939; Bastien and Campbell, 1992), direct experimental evidence supporting their causal impact on memory is currently lacking.

Advanced approaches employing auditory stimuli targeting the up-phase of ongoing slow waves (referred to as up-PTAS) have consistently demonstrated significant enhancements in the consolidation of verbal declarative memory (Ngo et al., 2013a, 2015; Papalambros et al., 2019, 2017; Ong et al., 2016; Leminen et al., 2017). However, none of these studies investigated the specific electrophysiological effects following stimulation that were associated with the observed improvements in memory consolidation. Moreover, there are indications that up-PTAS applied as trains of stimuli elicits an initial KC-like response, followed by a prolonged increase in slow-wave activity (SWA; spectral power between 0.5 and 4 Hz; Huwiler et al., 2022; Krugliakova et al., 2022). These findings highlight the inherent difficulties involved in studying the isolated effects of KCs in human research.

To evoke KCs in isolation, a promising approach is down-PTAS, which conceptually evokes KCs in a more restricted manner. With down-PTAS, auditory stimuli are presented specifically at the negative peak or descending slope of slow waves, corresponding to the beginning of cortical off-periods (Vyazovskiy et al., 2009; Crunelli et al., 2012). The limited studies employing down-PTAS during sleep suggest that auditory stimuli presented during cortical off-states may prematurely transition neuronal networks into on-periods, disrupting cortical bistability and impeding the occurrence of later slow waves (Fattinger et al., 2017; Moreira et al., 2021; Ngo et al., 2013a; Sousouri et al., 2022). Therefore, any observed increase in SWA following down-PTAS (as reported in Huwiler et al., 2022) could likely be attributed to evoked KCs.

Especially in stimulation protocols that aim to maximize the number of stimuli, such as those that utilize shorter inter-stimulus intervals, down-PTAS may be a more suitable approach for studying the isolated effects of KCs compared to random stimulation. This is because down-PTAS reduces the likelihood of inadvertent up-PTAS. However, current evidence on the impact of down-PTAS on declarative memory consolidation remains limited (Ngo et al., 2013a).

Following this rationale, this study aimed to investigate the role of evoked KCs in declarative memory consolidation through a two-step approach. Firstly, we sought to validate our assumption regarding the differential slow-wave response profiles of up- and down-PTAS by reanalyzing data from a previous study (Sousouri et al., 2022, see methods). Our findings corroborate that both up-PTAS and down-PTAS elicit a similar initial KC-like response, while only up-PTAS is followed by a sustained slow-wave response. The sustained slow-wave response was absent following down-PTAS.

Secondly, we proceeded to investigate the impact of down-PTAS on two specific domains of declarative memory (verbal and spatial) as well as alertness. Our findings revealed that experimentally evoked KCs, along with enhanced cross-frequency coupling between slow waves and spindles (a characteristic feature of KCs), were associated with significant improvements in overnight verbal memory consolidation. These results provide direct experimental evidence supporting a causal relationship between evoked KCs and the process of declarative memory consolidation in humans. Importantly, the use of down-PTAS minimized the potential interference of other slow-wave responses, allowing us to attribute the observed memory enhancements specifically to the effects of evoked KCs.

Results

Slow-wave response profiles of up- and down-PTAS

First, we tested our assumption that up- and down-PTAS result in different slow-wave response profiles. For this purpose, we reanalyzed high-density (hd-) EEG recordings (128 channels) of twelve participants, which were collected as part of a previous study (see methods). In short, participants underwent three experimental nights: two stimulation nights (STIM; one with up-PTAS, the other with down-PTAS), and a third night

without stimulation (SHAM; all randomized and counterbalanced). In the SHAM night, stimulation flags were saved without presenting actual tones. Stimuli (50 ms pink noise) were presented during NREM sleep (inter-stimulus interval (ISI) ≥0.5 s) in an ON|OFF window design: ON windows (6 s), allowing stimulation, took turns with OFF windows (6 s), withholding stimulation.

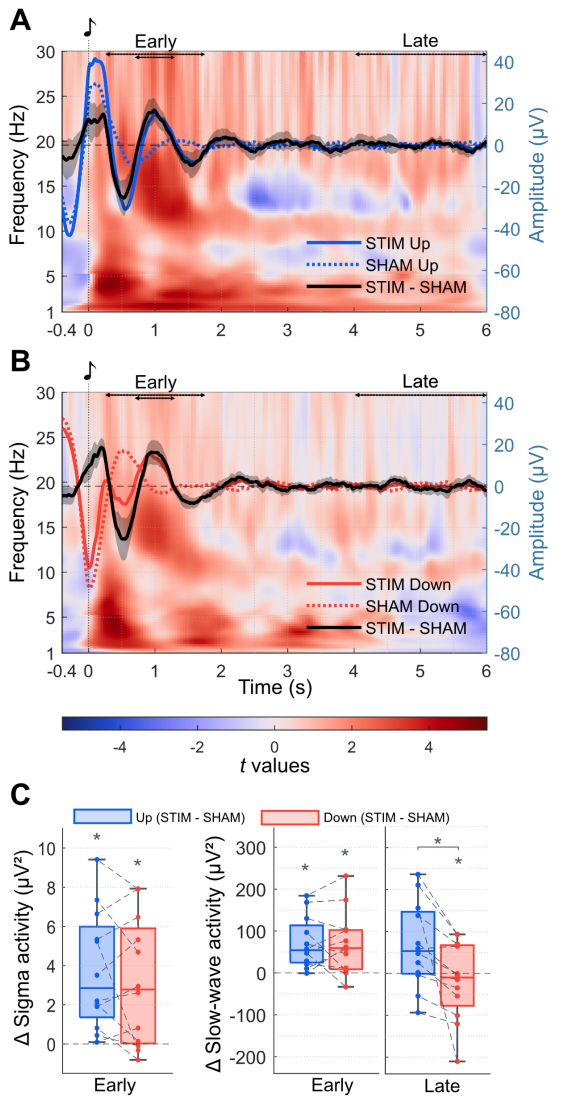

Fig. 1. Comparison of early and late responses between up- and down-PTAS. A) Auditory evoked potential (AEP, mean ± 95% CI; right y-axis) following up-PTAS and SHAM stimulation, time-locked to the initial stimulus of a given stimulation (ON) window (0 s). EEG data of channel FCz is displayed. The background illustrates the event-related spectral potential (ERSP; left y-axis) comparison with SHAM (paired *t* test). Dotted arrows on top signify time periods utilized for statistical comparisons in (C). The illustrated AEP and ERSP were computed using data from all windows regardless of the number of stimuli. **B)** Same as (A) for a night with down-PTAS. **C)** Mean sigma activity (12 – 16 Hz; left) and slow-wave activity (1 – 4 Hz; right) averaged over all channels. The early slow-wave (0.25 – 1.75 s) and sigma response (0.75 – 1.25 s) suggest a K-Complex-like response following both up- and down-PTAS. The later slow-wave response (4 – 6 s) is significantly stronger after up-PTAS compared to down-PTAS (paired *t* test).

Auditory evoked potential

We evaluated the phase-locked slow-wave response for both stimulation paradigms by computing the auditory evoked potential (AEP) time-locked to the first stimulus of a given ON window. Averaging the EEG of one fronto-central channel (FCz), the location where the largest AEP can be expected, revealed a pronounced AEP compared to SHAM after both up- (**Fig. 1A**) and down-PTAS (**Fig. 1B**). The AEP was statistically indistinguishable between stimulation paradigms ($p \geq .459$ for all sample points, FDR corrected), emphasizing the striking similarity between the initial phase-locked response observed in both stimulation approaches.

Early slow-wave response

Slow-wave response profiles were further characterized by comparing slow-wave and sigma activity levels at different periods in time (**Fig. 1C**, refer to **Fig. 1A & B** to see the whole time-frequency spectrum). The analysis was performed separately for windows with few (1 – 4) and many (5 – 9) stimuli, as the number of stimuli relates directly to SWA levels present at times of stimulation. SWA levels, in turn, have been shown to impact the resulting slow-wave response upon stimulation (Lustenberger et al., 2022).

Compared to SHAM, early SWA averaged over all channels (1 – 4 Hz; STIM−SHAM; 0.25 – 1.75 s after stimulus onset) in windows with few stimuli was significantly larger following both up-PTAS, $t(11) = 4.10$, $p = .002$, $d = 0.63$, and down-PTAS, $t(11) = 3.19$, $p = .009$, $d = 0.61$ (**Fig. 1C**, middle panel). This initial response was indistinguishable between stimulation paradigms, $t(11) = 0.16$, $p = .877$, $d = 0.03$.

Similarly, sigma activity levels (12 – 16 Hz; STIM−SHAM; 0.75 – 1.25 s after stimulus onset) were increased after both up-PTAS, $t(11) = 4.30$, $p = .001$, $d = 1.04$, and down-PTAS, $t(11) = 3.33$, $p = .007$, $d = 0.85$ (**Fig. 1C**, left panel). No statistical difference was observed between stimulation paradigms, $t(11) = 0.99$, $p = .342$, $d = 0.18$. Importantly, all findings related to the early slow-wave and sigma response remained consistent when considering all windows regardless of the number of stimuli.

These results provide further evidence that both stimulation paradigms evoke a similar initial slow-wave response. Furthermore, the presence of a subsequent sigma response that follows the initial slow-wave response suggests a potential involvement of evoked KCs in driving the initial slow-wave response (Halasz, 1993; Krugliakova et al., 2022).

Late slow-wave response

Next, at the end of stimulation windows (4 – 6 s after stimulus onset), SWA was compared between stimulation paradigms in windows with numerous stimuli (**Fig. 1C**, right panel). When compared to SHAM, SWA was exclusively enhanced after up-PTAS, $t(11) = 2.25$, $p = .046$, $d = 0.19$, but not after down-PTAS, $t(11) = -0.68$, $p = .509$, $d = -0.06$. Furthermore, SWA (STIM−SHAM) after up-PTAS was significantly larger compared to down-PTAS, $t(11) = 2.99$, $p = .012$, $d = 0.81$.

To summarize, our findings highlight the distinct dynamics of up- and down-PTAS in relation to slow-wave responses. Both types of PTAS can elicit a robust initial response, potentially driven by evoked KCs. However,

the sustained enhancement of SWA occurring later in the stimulation window appears to be exclusive to up-PTAS.

Effects of down-PTAS on EEG and memory

Building on these findings, we set out to examine the potential link between the initial KC-like response and declarative memory consolidation by applying down-PTAS in a new sample. Hd-EEG recordings from 14 participants were analyzed. Participants underwent two experimental nights, one with down-PTAS (STIM), the other without stimulation (SHAM; randomized and counterbalanced). Stimuli (50 ms pink noise) were presented during NREM sleep (ISI $\geq$0.5 s) in 16 s ON and 8 s OFF windows, following the signal of a target electrode next to C3 (see methods).

Evidence for an evoked K-complex-like response

Having observed KC-like features in the EEG response to the initial stimulus of a stimulation window (**Fig. 1**), we sought additional evidence to support the KC-like nature of this response. For this purpose, we first evaluated the AEP, specifically focusing on the N550 component, which is deemed essential for classifying a response as KC-like (Gora et al., 2001).

Auditory evoked potential and N550

Averaging the EEG of one fronto-central channel (FCz) time-locked to the first stimulus demonstrated a prominent AEP compared to SHAM ($p < .05$, FDR corrected; **Fig. 2A**). The AEP exhibited all classical sleep AEP components (P200, N350, N550 and P900). When identifying the N550 component in channel FCz and evaluating its amplitude across channels, it was found to be largest over fronto-central regions ($p < .05$, cluster corrected; **Fig. 2B**), matching the anticipated topography of the N550 component of KCs (Cote et al., 1999).

Event-related spectral potential

Alongside the close relationship between KCs and sleep spindles, it has been noted that evoked KCs exhibit a distinctive spectral profile, featuring increases in the theta, alpha, sigma, and beta bands (Halasz, 1993). To evaluate this spectral profile, the event-related spectral potential (ERSP) was computed time-locked to the first stimulus within a predefined frontal region of interest (ROI). The analysis revealed a significant increase in sigma activity (12 – 16 Hz) around 0.9 – 1.5 s after stimulus presentation in comparison to SHAM ($p < .001$, cluster corrected, 99.9th percentile; **Fig. 2C**). Additionally, the stimuli evoked an early response in the low slow-wave band (1 – 1.5 Hz) around 0.7 – 1.3 s, as well as in the high slow-wave (2 – 4 Hz), theta (4 – 8 Hz) and beta band (17 – 23 Hz) around 0.3 – 0.7 s after stimulus presentation. Further topographic analyses of the low slow-wave and sigma responses revealed that the increase in SWA and sigma activity was global ($p < .05$, cluster corrected), yet varied topographically in terms of effect sizes (topographies in **Fig. 2C**). The increase in low SWA was most pronounced over fronto-central regions (maximum Hedges's g = 1.88), while the increase in sigma activity was greatest over parietal areas (maximum Hedges's g = 3.65), aligning well with the expected topography of the slow-wave and spindle components of evoked KCs.

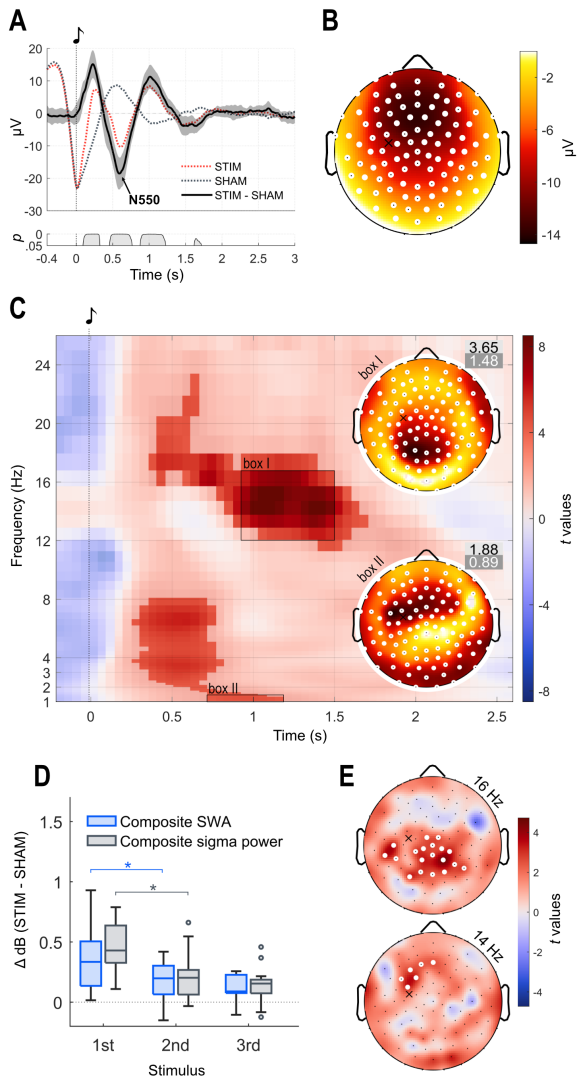

Fig. 2. Indications for a K-complex-like response. In all panels, time 0 s corresponds to the onset of the first stimulus. **A)** Auditory evoked potential (AEP, mean ± 95% CI) of channel FCz. The bottom panel displays significant differences between conditions (paired *t* test, FDR corrected). **B)** Topography of the difference in N550 amplitude between conditions (STIM −SHAM). The latency of the N550 component was determined individually for each night, based on the event-related potential (ERP) of the channel average in a predefined frontal region of interest (ROI). White dots represent electrodes with significant differences between conditions (paired *t* test, cluster corrected); the black cross indicates the target electrode. **C)** Normalized (frequency-wise, by the trial average of the entire time window) event-related spectral potential (ERSP). The ERSP of the channel average in a predefined frontal ROI is shown. Highlighted tiles signify significant differences between conditions (paired *t* test, cluster corrected). The topography of effect sizes (Hedge's G) of the mean sigma (box I; 900 – 1500 ms; 12 – 16 Hz) and low slow-wave (box II; 700 – 1300 ms; 1 – 1.5 Hz) response is depicted in the topography of box I and II, respectively. **D)** Composite slow-wave (700 – 1300 ms; 1 – 1.5 Hz; in blue) and sigma response (900 – 1500 ms; 12 – 16 Hz; in gray) after each of the first three stimuli within a stimulation window. The slow-wave and sigma response was largest after the first stimulus (paired *t* test). **E)** Topography of the difference in phase-power coupling (z-standardized modulation index: zMI) between conditions (STIM −SHAM; paired *t* test, cluster corrected). Stimulation-induced coupling between 16 Hz spindles and 1 Hz slow waves (top), as well as between 14 Hz spindles and 2.5 Hz slow waves (bottom) is illustrated.

Response after subsequent stimuli

As KCs exhibit a refractory period (Kurella et al., 1992), the largest increase in spectral power, if due to evoked KCs, would be expected to occur after the first

tone of a stimulation window compared to subsequent tones. To investigate this, the increase in low SWA and sigma activity in response to the first two stimuli of the stimulation window were compared in a predefined frontal ROI. Both the slow-wave, $t(13) = 3.02$, $p = .010$, $d = 0.71$, and sigma response, $t(13) = 4.66$, $p < .001$, $d = 1.05$, were stronger after the first stimulus compared to the second (**Fig. 2D**). Similarly, the amplitude of the N550 component in channel Fz was stronger after the first stimulus, $t(13) = 4.40$, $p = .001$, $d = 0.98$ (data not shown).

Cross-frequency coupling between slow waves and spindles

Consistent with existing literature (e.g., Krugliakova et al., 2020), the observed enhancement in sigma activity occurred 0.9 – 1.5 s after stimulus presentation (**Fig. 2C**) and coincided with the slow P900 component of the AEP (**Fig. 2A**). This co-occurrence suggests a stimulation effect on the nesting of sleep spindles within slow waves. As KCs frequently precede sleep spindles (Landwehr, 2007), an enhancement in cross-frequency coupling between slow waves and spindles would provide further evidence supporting the KC-like nature of the evoked response.

To explore this, phase-power coupling between slow waves (1 – 4 Hz, 0.5 Hz steps) and sleep spindles (11 – 16 Hz, 1 Hz steps) was topographically assessed by computing the z-standardized modulation index (zMI) within 0 – 2 s after the first stimulus within a given ON window, separately for each channel. Interestingly, the spatial pattern of stimulation-induced coupling between slow waves and sleep spindles was found to be dependent on the specific frequency band of each (two examples are depicted in **Fig. 2E**). More specifically, the coupling between spindles (12 – 14 Hz) and faster slow waves (2 – 4 Hz) was increased in a fronto-central cluster of 6 – 11 channels after stimulation ($p < .05$, cluster corrected; **Supplementary Fig. 3)**. This effect tended to lateralize towards the stimulation electrode.

Faster spindles (14 – 16 Hz), on the other hand, were more strongly coupled to slower slow waves (1 – 1.5 Hz, **Supplementary Fig. 3)**. The coupling was increased in a parietal cluster of 17 – 19 channels with 1 Hz waves, and in a central cluster of 9 – 13 channels with 1.5 Hz waves ($p < .05$, cluster corrected). Overall, these findings suggest that the initial evoked response led to enhanced coupling between different spindle and slow-wave frequencies in a topographically distinct manner.

Spectral power changes throughout and beyond the stimulation window

The preceding analyses indicated that the first stimulus within stimulation windows robustly evokes a KC-like response. However, the effects of stimuli later in the stimulation window have not been fully explored. Hence, in a next step, we analyzed the EEG response throughout the entire ON|OFF window, thereby focusing on changes in SWA.

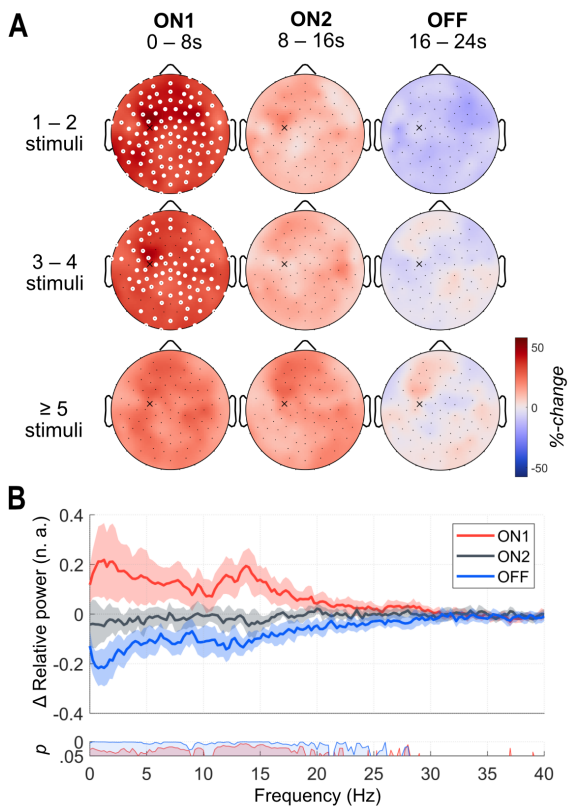

Fig. 3. Spectral power in ON and OFF windows. A) Topography of absolute slow-wave activity (SWA; 1 – 4.5 Hz) within 8 s window snippets (ON1, ON2, OFF) containing few (1 – 2), medium (3 – 4) and many ($\geq$5) stimuli within the first 6 s in ON1. White dots represent electrodes with significant differences between conditions (paired *t* test, cluster corrected); the black cross indicates the target electrode. **B)** Relative power spectral density (PSD, mean $\pm$ 95%CI) of 8 s window snippets (ON1, ON2, OFF) belonging to ON|OFF-window pairs which had 1 – 2 stimuli within the first 6 s in ON1. PSD values within window snippets are normalized to the channel average of the entire ON|OFF window (window- and frequency-wise). Relative PSD values thus indicate a redistribution of PSD within windows. The average PSD of all electrodes is depicted. Bottom panel displays significant differences between conditions (paired *t* test, FDR corrected).

SWA response within stimulation windows

The 16 s ON and 8 s OFF windows were divided into equally long windows of 8 s duration in order to compare SWA (1 – 4.5 Hz) between conditions (STIM–SHAM). Consistent with the previous findings of a KC-like response to the first stimulus, SWA was globally increased at the beginning of stimulation windows (ON1; $p < .05$, cluster corrected; data not shown) but not later on (ON2 & OFF; all $p < .05$). To investigate a potential dose-response relationship and account for ongoing SWA during stimulation, we further divided ON|OFF-window pairs based on the number of stimuli presented within the first 6 s of stimulation. Intriguingly, the observed increase in SWA during ON1 was most pronounced in stimulation windows with 1 – 2 stimuli, followed by those with 3 – 4 stimuli, and was completely absent in windows with 5 or more stimuli ($p < .05$, cluster corrected; **Fig. 3A**). These results, while initially surprising, can be explained by the elevated arousal threshold during deeper sleep stages (Neckelmann and Ursin, 1993). It is during lighter sleep stages that soft stimuli are more likely to elicit KCs.

The limited duration of SWA enhancements already suggests the temporal specificity of the stimulation

effect. Comparing the time spent in different sleep stages across condition (STIM−SHAM) confirmed the absence of any significant alterations in sleep architecture (paired t test, FDR corrected, all $p \geq .05$; **Supplementary Fig. 2D**). Additionally, no difference was observed in overnight SWA, as indicated by mean SWA across all NREM epochs (paired t test, cluster corrected, all $p \geq .05$; **Supplementary Fig. 2A – C**).

Re-distribution of spectral power within ON|OFF window pairs

To investigate whether the increase in spectral power at the beginning of stimulation windows was specific to SWA, we assessed the redistribution of spectral power across the 0 – 40 Hz frequency range. For a given frequency, PSD values within ON1, ON2, and OFF windows were normalized by the channel average PSD of the respective entire ON|OFF window and compared between conditions (STIM−SHAM). Most frequencies up to 18 Hz, with the exception of alpha activity (∼10 Hz), were redistributed towards ON1 and away from OFF (**Fig. 3B**). These findings suggest that the early KC-like response not only enhances SWA compared to SHAM, but also causes a shift in SWA, theta, and sigma activity towards the beginning of stimulation windows, where evoked KCs are concentrated.

Improved verbal declarative memory consolidation

Although down-PTAS induced a prominent EEG response resembling a KC, its functional significance remains unclear. To further investigate this, we examined the effect of down-PTAS on verbal and spatial declarative memory consolidation and alertness. Memory was assessed using an associated word-pair memory task (40 word-pairs; **Supplementary Fig. 6**) and an object-location task (15 object-locations; **Supplementary Fig. 7**). Participants learned the word-pairs and object-locations before sleep. Recall of learned items was performed in the evening (directly after learning, *immediate retrieval*) and in the morning (after sleep, *delayed retrieval*). The difference in recalled items between the two time points was calculated as the score for overnight memory consolidation. Additionally, participants learned and directly recalled a new list of 40 word pairs in the morning to asses their encoding capabilities after down-PTAS (illustration of procedure in **Supplementary Fig. 5D & E**).

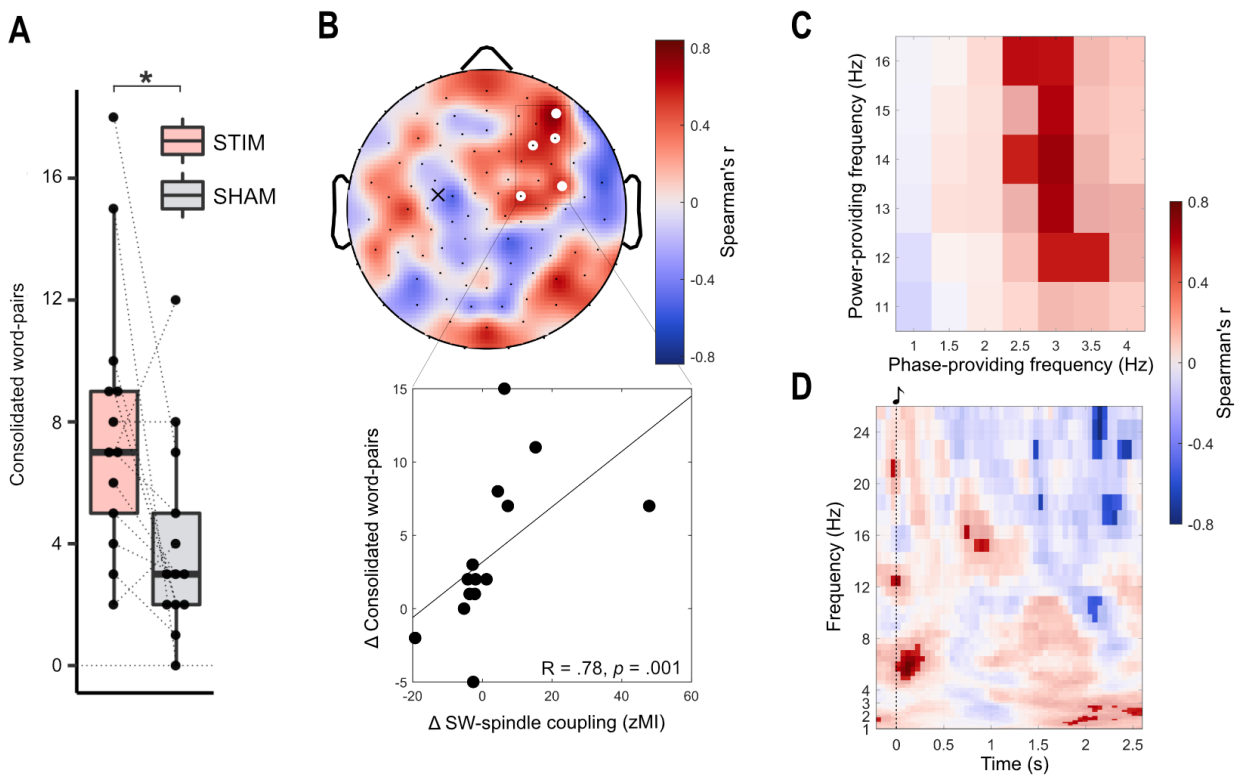

Fig. 4. Verbal memory consolidation. A) Overnight memory improvement in the associated word-pair memory task (morning − evening) after a night with (STIM) and without auditory stimulation (SHAM). Dots represent the performance of single participants. **B)** (Top) Spearman's rank correlation coefficient between the number of consolidated word-pairs (STIM−SHAM) and slow-wave-spindle coupling (z-standardized modulation index (zMI)) between 2.5 Hz slow waves and 14 Hz spindles (STIM−SHAM). White dots represent electrodes with significant correlations (cluster corrected); the black cross indicates the target electrode. (Bottom) Mean zMI of significant electrodes in relation to the number of consolidated word-pairs. Black dots represent single participants. **C)** Spearman's rank correlation coefficient between the number of consolidated word-pairs (STIM−SHAM) and the average slow-wave-spindle coupling (zMI) of channels belonging to a pre-defined region of interest around F4 (STIM−SHAM). Emphasized tiles represent coupled frequencies that significantly correlated with the observed improvement in memory (all $p < .05$, cluster corrected, 97.5th percentile). **D)** The number of consolidated word-pairs (STIM−SHAM) was correlated with each pixel of the ERSP (STIM−SHAM). The ERSP was computed for the time after the first stimulus, taking the channel average of a frontal region of interest. Highlighted tiles indicate a significant correlation (not cluster corrected).

For the associated word-pair task, auditory stimulation significantly improved overnight verbal memory consolidation, $t(12) = 2.58$, $p = .023$, $d = 0.72$ (**Fig. 4A**). No significant differences were found for encoding capabilities of new word-pairs, $t(12) = 0.52$, $p = .606$, $d = 0.15$ (**Supplementary Fig. 5A**), or for the consolidation of object-locations (**Supplementary Fig. 5B**), $t(11) = 0.00$, $p = 1.000$, $d = 0.00$.

Unchanged alertness

To investigate the impact of down-PTAS on alertness, participants underwent a simple reaction time task before and after sleep. Both phasic and tonic alertness were assessed (see methods). The standard deviation in reaction times measured in the morning was subtracted from those measured in the evening to assess alertness. Our results indicate that down-PTAS had no significant effect on either phasic, $t(12) = -0.23$, $p = .823$, $d = -0.06$, or tonic altertness, $t(12) = -0.24$, $p = .814$, $d = -0.07$ (**Supplementary Fig. 5C**). These results remain consistent when evaluating alertness based on the average reaction times instead of the standard deviation.

Positive relationship between cross-frequency coupling and memory improvements

Given the growing body of evidence supporting the involvement of cross-frequency coupling between slow waves and spindles in sleep-dependent memory processes, we aimed to investigate the relationship between enhanced coupling and improved verbal declarative memory consolidation following down-PTAS using Spearman's rank correlation coefficient. Remarkably, stimulation-induced coupling between 14 Hz spindles and 2.5 Hz slow waves (STIM−SHAM) correlated significantly with the improvement in verbal memory consolidation (STIM−SHAM) in a right frontal cluster of 5 channels ($p < .05$, cluster corrected; mean $r(12) = 0.78$, mean $p = .001$; **Fig. 4B**). The positive relationship provides a possible mode of action for how evoked KCs may interact with declarative memory consolidation.

Furthermore, to enhance statistical power, cross-frequency coupling (STIM−SHAM) averaged over channels belonging to one of nine pre-defined ROIs (**Supplementary Fig. 8)** was correlated with the improvement in verbal memory consolidation (STIM−SHAM). Consistent with the results obtained on the topographical level, stimulation-induced coupling in a region around F4 correlated significantly in a cluster of 8 coupled frequencies ($p < .05$, cluster corrected; mean $r(12) = 0.593$, mean $p = .027$, **Fig. 4C**). Interestingly, when examining the frequency cluster, the specific slow-wave frequency to which spindles coupled, particularly 2.5 – 3.5 Hz slow waves, appeared to hold significant importance for successful memory consolidation.

Meaningful relationship between spectral power profile and memory improvements

In an additional exploratory analysis, we investigated the potential relationship between the spectral power profile following stimulation and the improvement in verbal memory consolidation. Interestingly, we observed a meaningful association between the two, although these results did not withstand cluster correction (**Fig. 4D**). A KC-like spectral signature, characterized by enhanced early theta activity (5 – 8 Hz between 0 and 0.25 s; max. $r(12) = 0.785$, $p = .001$), sigma activity (14 – 17 Hz between 0.7 and 1 s; max. $r(12) = 0.628$, $p = .016$), and subsequent SWA (1 – 3 Hz between 1.75 and 2.5 s; max. $r(12) = 0.631$, $p = .016$) demonstrated positive correlations with improvements in verbal memory consolidation (STIM−SHAM). Conversely, increased beta activity (18 – 25 Hz, between 2 and 2.5 s; min. $r(12) = -0.792$, $p = .001$) was negatively correlated, indicating that signs of arousal are counterproductive for verbal memory consolidation.

Discussion

By experimentally inducing KC-like EEG responses and concurrently observing a significant enhancement in the consolidation of verbal declarative memory, our study establishes compelling evidence of a causal relationship between evoked KCs and the consolidation of verbal declarative memory in healthy adults.

Our results demonstrate that down-PTAS successfully improved the consolidation of verbal declarative memory. In the EEG, we observed a robust KC-like response, particularly in response to early tones within the stimulation window. Additionally, the KC-like response was accompanied by increased cross-frequency coupling between slow waves and sleep spindles in a topographically distinct manner. Importantly, this augmented coupling, specifically when observed in the right frontal region, was positively correlated with the facilitation of consolidation for previously learned word-pairs.

The missing link between auditory stimulation and improved memory consolidation

Despite numerous studies demonstrating memory enhancements after auditory stimulation (reviewed in Harrington and Cairney, 2021; Zhang and Gruber, 2019), none have thoroughly examined the electrophysiological response following stimulation that could elucidate the underlying mechanisms responsible for the observed improvements in memory consolidation. In addressing this critical gap, our study makes a significant contribution by

1. implementing a stimulation approach, i.e., down-PTAS, that effectively isolates evoked KCs while minimizing confounding slow-wave responses,

2. conducting a comprehensive investigation of the relationships between EEG responses following stimulation and the observed improvements in memory consolidation.

To the best of our knowledge, this study represents the first direct experimental evidence supporting the specific causal role of KCs in verbal memory consolidation in healthy adults.

The role of K-complexes in memory consolidation

By demonstrating a significant correlation between enhanced cross-frequency coupling between slow waves and sleep spindles and improved memory recall, our study provides insights into how evoked KCs may contribute to sleep-dependent memory consolidation.

In the framework of the influential hippocampal memory indexing theory (Teyler and DiScenna, 1986) and the current active system consolidation concept (Klinzing et al., 2019), memory consolidation unfolds as a two-step process. First, new information is thought to be encoded in both the hippocampus and neocortex, eventually becoming solely dependent on the neocortex. Although the precise neuronal mechanisms underpinning this process remain elusive, substantial evidence from electrophysiological studies supports that the synchronization between slow waves, sleep spindles, and hippocampal ripples, along with their temporal hierarchy, reflects the hippocampal-neocortical dialogue crucial for memory consolidation (reviewed in Takehara-Nishiuchi, 2021).

Hence, our data supports the conceptual framework that evoked KCs facilitate memory consolidation during sleep by actively participating in the hippocampal-neocortical dialogue which strengthens neuronal connections underlying the memory trace (reviewed in Genzel et al., 2014).

The importance of cross-frequency coupling in a right frontal region

The high spatial resolution of our EEG recordings, with 128 channels, allowed us to conduct a detailed examination of topographic differences in cross-frequency coupling following stimulation and its relationship to memory consolidation.

Our results showed that specifically the coupling in a right frontal region was associated with the observed enhancement in verbal memory consolidation. Although the precise neuronal origin of the right frontal increase remains speculative, previous research has implicated the medial prefrontal cortex (mPFC; Maingret et al., 2016), which receives monosynaptic input from the hippocampus (Ferino et al., 1987), and the medial temporal lobe (MTL; Alvarez and Squire, 1994; Geva-Sagiv et al., 2023) in memory consolidation processes. FMRI studies investigating the neural correlates during encoding and retrieval processes of associated word-pairs revealed the activation of bilateral prefrontal cortical areas (Mottaghy et al., 1999), with the right mPFC showing particular sensitivity to familiar stimuli that had been presented before the scanning session (Fletcher and Dolan, 1999). Given that the word-pairs used in our associated word-pair task consisted of everyday words, the observed importance of coupling in the right frontal region may be attributed to the familiarity of the stimulus material.

Furthermore, a recent study combining fMRI and EEG revealed increased activation in parahippocampal and frontal cortical regions during coupled slow-wave-spindle events compared to isolated spindle events detected in the scalp EEG (Baena et al., 2023). These findings further emphasize the association between cross-frequency coupling observed in the surface EEG and the simultaneous engagement of the hippocampus and neocortex during sleep.

The importance of coordinated communication

Despite the absence of overnight changes of SWA or sleep architecture, we observed a significant improvement in verbal memory recall following a night of down-PTAS. The extent of enhancement in memory recall positively correlated with the increased coupling between slow waves and sleep spindles. These findings are consistent with a recent study involving electrical stimulation in the MTL of patients with pharmacoresistant epilepsy (Geva-Sagiv et al., 2023), where no significant increase in the total number of hippocampal ripples detected in the MTL was observed. However, a positive correlation was found between the enhanced coupling of neocortical slow waves with hippocampal ripples and the improvement in visual memory consolidation. These results could explain how down-PTAS facilitates overnight memory consolidation; rather than increasing overall SWA, down-PTAS may have orchestrated the precise timing of hippocampal-neocortical communication as implicated by enhanced cross-frequency coupling after stimulation.

The importance of coupling with faster slow waves

Interestingly, we observed a significant positive correlation between the enhanced coupling in the right frontal ROI around F4 and the consolidation of verbal memory, particularly when spindles nested with faster slow waves in the range of 2.5 – 3.5 Hz. It is worth noting that previous studies have reported a robust coupling between hippocampal ripples and 3 Hz slow waves recorded within the hippocampus, which adds to the intriguing nature of this finding (Staresina et al., 2015; Ngo et al., 2020). However, it remains speculative at this stage whether the nesting within 3 Hz slow waves at the scalp level is associated with the modulation of ripples in the hippocampus. Further research is needed to explore this potential relationship.

Selective functional role of K-complexes

The specific involvement of frontal regions may provide an explanation for the selective enhancement of verbal memory consolidation following KC induction. In our study, the positive outcome was selective for verbal declarative memory consolidation and did not extend to visuo-spatial memory consolidation, verbal encoding capabilities, or alertness. These findings highlight the selectivity of the impact of evoked KCs and is consistent with the concept that the mechanisms underlying the consolidation of different domains of memories varies (Walker, 2005). Consequently, our results suggest that KCs may play a more prominent role in verbal memory consolidation compared to other cognitive functions such as visuo-spatial memory or alertness.

Topographic investigation of cross-frequency coupling

Usually, cross-frequency coupling is evaluated by examining the embedding of spindles within slow waves

of a specific frequency range, typically within the SO range (e.g., Cox et al., 2014). However, in our data, the systematic investigation of cross-frequency coupling between slow waves and spindles at different frequencies revealed that faster spindles (14 – 16 Hz) preferred to nest within slower slow waves (1 – 1.5 Hz), while slower spindles (11 – 14 Hz) demonstrated a preference for faster slow waves (2 – 4 Hz). The functional consequence of these frequency-specific interactions remain elusive at this point.

Locally enhanced cross-frequency coupling

Interestingly, the topographic pattern of the observed enhancement in coupling exhibited variability based on the specific frequencies that were involved. Notably, the coupling between spindles in the frequency range of 12 – 14 Hz and slow waves in the range of 2 – 2.5 Hz exhibited a pronounced concentration around the target electrode C3. This finding aligns with the results of a previous study that utilized up-PTAS with different stimulation parameters (Krugliakova et al., 2020), indicating a potential interaction between evoked KCs and endogenously generated neuronal activity in a phase-dependent manner.

Contradicting studies

It is relevant to mention that our findings contradict an earlier study (Ngo et al., 2013b) that reported no improvements in either memory consolidation or SWA levels following down-PTAS. A plausible explanation for this discrepancy lies in the difference in the stimulation protocol used between the two studies. Upon investigating the relationship between the spectral power profile following stimulation and the enhancement in memory performance in our data, we discovered evidence suggesting that specific spectral characteristics associated with KCs, such as elevated SWA, theta, and sigma power, were positively correlated with the observed improvements in memory. Conversely, increased beta activity linked to arousal displayed a negative correlation with memory performance.

It is worth noting that Ngo et al. 2013b observed an enhancement in SWA and memory recall when using up-PTAS with a two-click design and an ISI of 1.075 seconds. However, when down-PTAS was employed with a reduced ISI of 0.55 seconds, potentially leading to electrophysiological states related to arousals, the enhancements in SWA and memory recall were absent. In our study, the median ISI ranged between 0.96 and 1.41 seconds within participants, with a mean ISI of 1.27 seconds across participants. Notably, the second stimulus therefore coincided with the time period of the robust spindle response (0.9 – 1.5 s), which is known to reduce sensory responsiveness during sleep (Lüthi, 2014). In the earlier study, however, only the long ISI of 1.075 seconds, but not the short ISI of 0.55 seconds, coincided with the time period of the spindle response.

Hence, while both studies likely evoked KCs, the relationship between KCs and arousals appears to be of importance in their functional role towards memory consolidation. This observation also aligns with the notion that KCs seem to have a dual functional role, as highlighted in the continuous discussion regarding their contribution to both arousal and sleep protection (Colrain, 2005).

Future applications

The successful application of PTAS with an appropriate stimulation protocol holds promise for improving verbal memory consolidation by evoking KCs. This approach appears particularly appealing not only in healthy individuals but also in patients with Alzheimer's disease, who commonly experience deficits in memory and a reduction in KC density (De Gennaro et al., 2017).

To successfully induce KCs during sleep, stimuli should be presented during sleep stages known to facilitate their generation, specifically targeting NREM sleep, including stage N2. The stimulus intensity should be salient enough to elicit KCs (Laurino et al., 2014) but also quiet enough to prevent awakenings and arousals. Sporadic breaks of stimulation (Roth et al., 1956; Kurella et al., 1992) with irregular ISIs (Johnson and Lubin, 1967) can facilitate KC generation.

Conclusions

By experimentally inducing KC-like EEG responses while minimizing other slow-wave responses and simultaneously observing improved verbal declarative memory consolidation in young healthy adults, this study provides compelling and direct evidence establishing a causal relationship between evoked KCs and the consolidation of verbal declarative memory. These findings align with prevailing theories on memory consolidation during sleep, therefore supporting the notion that evoked KCs play a pivotal role in coordinating the precise timing of cortical slow waves, thalamic spindles, and possibly even hippocampal ripples. We support the proposition that evoked KCs make a substantial contribution to the consolidation of memory during sleep likely through the active participation in the communication between the hippocampus and neocortex.

Acknowledgments

We extend our gratitude to every member of Prof. Reto Huber's lab and the entire SleepLoop consortium for their constructive feedback and insightful discussions. Special thanks are due to Maria E. Dimitriades for her valuable discussions and meticulous proofreading. We further express our sincere gratitude to Simone Accascina for providing invaluable technical assistance for our custom recruiting website. We express our appreciation to Cécile Abati, Tamara Weil, Paulina Schmiedeberg, Nicole Meier, Vanessa Kasties, Veronika Voskresenska, and Gila Norup for their valuable contributions to data collection. Lastly, we are grateful to all the study participants for their participation and cooperation. This work was supported by the Swiss National Science Foundation (SNF) under grant number 320030_179443 and is

part of the HMZ Flagship grant «SleepLoop» under the umbrella of «Hochschulmedizin Zürich», Switzerland.

Author contributions

Author contributions follow the Contributor Roles Taxonomy. **Conceptualization**: SL and RH; **Data curation**: SL, SSch, and MM (new data); EK, JS, SL, SS (existing data) **Formal analysis**: SL (new & existing data) and EK (existing data); **Funding aquisition**: RH; **Investigation**: SL, SSch, and MM (new data); EK, JS, SL, and SS (existing data); **Project administration**: SL and RH; **Resources**: RH; **Software**: MLF, GP, GS, WK, SS, SL, and MM; **Supervision**: RH; **Visualization**: SL; **Writing**: SL (original draft); all authors (review and editing).

Declaration of interests

RH and WK are founders and shareholders of Tosoo AG, a company developing wearables for sleep electrophysiology monitoring and stimulation. Tosoo AG did not contribute in any form to the work presented in this manuscript. The remaining authors declare no competing interests.

Methods

Reanalysis of existing data

To investigate the hypothesis that up- and down-PTAS lead to distinct profiles of slow-wave responses, we conducted a re-analysis of hd-EEG recordings from a subset of twelve out of 18 participants aged between 18.38 and 26.69 years (mean±sd = 23.83±1.51 years; 6 male, 6 female). Participants had previously undergone the study procedure comprising three experimental nights: one with up-PTAS, one with down-PTAS, and one without stimulation (SHAM) (Sousouri et al., 2022). The data collected after a night with up-PTAS (Krugliakova et al., 2020; Sousouri et al., 2022) and down-PTAS (Sousouri et al., 2022) had been previously analyzed for different research purposes.

EEG analyses

The auditory evoked potential was computed as described later. Time-frequency analyses were performed using Hanning-window-tapered wavelets and sliding time windows with a time step of 0.02 seconds. The length of the sliding window was adjusted to ensure that it would fit 4 full cycles for frequencies between 0.75 and 5 Hz, and 6 full cycles for frequencies between 5 and 30 Hz. The average-referenced EEG data was aligned to the onset of the first stimulus within an ON window and used as input for Fieldtrip's *ft_freqanalysis()* function with the *mtmconvol* option. ON windows were categorized based on the number of stimuli occurring within each window, either between 1 and 4 stimuli or between 5 and 9 stimuli. The average ERSP over ON windows was computed and stored for further analysis.

Collection of new data

New data was collected employing down-PTAS to investigate the role of evoked KCs on two domains of declarative memory consolidation. Additionally, the selectivity of KCs was investigated in relation to alertness.

Participants

A total of 17 participants were initially recruited, with 14 (4 male, 10 female) successfully completing the study. All participants were right-handed and aged between 18.38 and 26.69 years (mean±sd = 23.25±2.53 years). Three participants dropped out due to reasons including disregarding bedtimes (N = 1), poor sleep efficiency (<70%, N = 1), and technical issues (N = 1).

All participants except for one were native Swiss-German speakers. Prior to the study, in an anonymous online-screening, all participants self-disclosed their medication-free status, low consumption of caffeine and alcohol, and abstinence from nicotine and other drugs. They also reported no personal or family history of neurological or psychiatric disorders, including sleep disorders. Participants affirmed themselves as good sleepers with an average chronotype and were excluded from the study if they had engaged in shift work, daytime napping, or traveled across more than two time zones within the previous 30 days.

The study was approved by the local ethics committee (Kantonale Ethikkommission Zürich, KEK-ZH, BASEC 2019-02134) and was conducted in adherence to the principles outlined in the Declaration of Helsinki. Written informed consent was obtained from all participants before their participation in the study. Data collection took place between August 2020 and April 2021.

Study design and procedure

Eligible participants initially followed a predetermined sleep schedule that matched their laboratory bedtimes for ∼7 days, with a range of 5 to 7 days, prior to both study nights. Bedtimes were recorded using daily sleep diaries and wrist actigraphy monitoring (Actiwatch Type AWL, CamNtech, Cambridge, UK).

Participants were permitted to consume a restricted amount (1 standard portion) of alcohol and caffeine up to 4 days before the experiment. Complete abstinence from alcohol and caffeine was required from that point until the day of the experiment. Participants documented their consumption of these substances and any medication through self-reports. On the day of the experiment, participants were instructed to refrain from activities known to affect sleep, such as sauna use or engaging in extreme sports.

A randomized, double-blind, crossover study design was employed, with each participant undergoing two experimental nights: a stimulation night (STIM) and a SHAM night (SHAM). The two nights were separated by a minimum of 5 days.

On the days of the experiment, participants arrived at the laboratory at 6:50 p.m. and completed a day-report questionnaire. Following the preparation of EEG (electroencephalogram), EMG (electromyogram), and ECG (electrocardiogram) recordings, a 3-minute resting-state EEG was recorded. Subsequently, participants performed four behavioral tasks (word-pairs, object-locations, alertness, finger-tapping task) between 8:30 and 9:45 p.m., in the specified order. Task motivation was assessed before each task. The object-location task was introduced starting from the 2nd participant, leading to 13 complete data sets. The finger-tapping task was only introduced starting from the 8th participant, which is why the data were not included in the analysis.

Sleep EEG recordings commenced at 10:30 p.m. with lights off. Auditory stimulation was initiated after 10 minutes of stable NREM (non-rapid eye movement) sleep was detected. Following an 8-hour sleep opportunity, lights were turned on at 6:30 a.m., and participants were immediately requested to complete a sleep report. At 7:15 a.m., which was 45 minutes after lights were turned on to minimize sleep inertia, resting-state EEG and all behavioral tasks were repeated. The total duration of the task session was approximately 1 hour. If participants indicated habitual earlier bedtimes, the schedule was advanced by 30 minutes.

Three weeks after each experimental night, the retrieval of both memory tests (word-pairs and object-locations) was repeated through video calls conducted with participants from their respective homes. This follow-up assessment allowed for the examination of long-term memory performance and retention beyond the immediate post-experimental period (data not included).

Behavioral tasks

Four behavioral tasks were administered in the study. These tasks included two declarative memory tests, one focused on verbal memory, the other on spatial memory. Additionally, an alertness and a motor-learning task (data not included) were used to assess different cognitive functions and abilities.

Associated word-pair memory task

Auditory presentation of words was conducted using PsychoPy (version 2020.1.3; Peirce et al., 2019) through the loudspeakers of a laptop. For the sake of test standardization, words-pairs had been previously recorded by the same person.

In the evening session, participants were tasked with learning a list of 40 word-pairs that were characterized by low emotionality and high tangibility (*encoding phase*, **Supplementary Fig. 5D**). Immediately following the encoding phase, participants were presented with only the first word of each word-pair and were required to recall the associated word within the pair without a specific time limit (*immediate retrieval*). If an incorrect response was provided, the full word-pair was presented again. The immediate retrieval process continued until participants successfully recalled at least 60% (24 word-pairs) of the word-pairs correctly. The experimenter assessed the accuracy of each response and

determined whether it was correct or false through a button press, ensuring accurate calculation of the 60% threshold.

In the morning session, participants were presented with the first word of each word-pair and were asked to recall the associated word (*delayed retrieval*). No feedback was provided during the delayed retrieval phase.

Afterwards, in the morning session, participants underwent a new encoding phase where they learned another set of 40 word-pairs (*new encoding*). Immediate retrieval of the newly learned word-pairs was conducted once without replaying falsely recalled word-pairs. No feedback was given during this process.

To assess long-term memory consolidation, delayed retrieval of word-pairs from the initial encoding phase in the evening session occurred three weeks after the experimental night. Participants performed the retrieval task from their homes via video call, and no feedback was provided during the retrieval session. This data is not presented.

Among the four lists (**Supplementary Fig. 6)**, lists 1 and 2 were consistently used during the evening encoding sessions, while lists 3 and 4 were exclusively used during the morning sessions. Specifically, list 1 was always followed by list 3, and list 2 was always followed by list 4. The word-pairs within each list were presented in a randomized order, while the assignment of lists was randomized across different conditions.

The inter-stimulus interval (ISI) between the words within a word-pair, starting from the voice play onset of the first word to the the onset of the second word, was set to 2 seconds. Additionally, the ISI between consecutive word-pairs, starting from the voice play onset of the second word to the onset of the first word of the next pair, was set to 5 seconds.

A pool of 160 word-pairs was utilized (**Supplementary Fig. 6)**, consisting of 112 word-pairs adopted from previous studies (32 from Marshall et al. 2006, 80 from Wilhelm et al. 2008, and 48 newly selected word-pairs from Hager and Hasselhorn 1994).

Object-location task

The object-pairs were assigned specific locations on a 5 x 6 checkerboard-pattern, consisting of 30 gray tiles separated by a white grid (**Supplementary Fig. 5E**). The experiment was implemented using Psychopy (version 2020.1.3; Peirce et al., 2019).

During the evening session, participants were instructed to learn the locations of 15 neutral day-to-day object-pairs (encoding phase). During the encoding phase, the first object of a pair was presented for a duration of 1 second. Subsequently, the second object of the pair was revealed, allowing participants to view the entire object-pair for an additional 3 seconds. The ISI between each object-pair presentation was set to 3 seconds.

The encoding process was conducted twice, with each presentation using a different randomized order of object-pairs. A separate practice session was not required. After encoding, participants have seen the location of each object-pair twice.

Following the encoding phase, participants were presented with only the first object and were required to click on the gray square corresponding to the location of the corresponding object-pair (immediate retrieval). There was no specific time limit imposed during this task. The location of the correct object-pair was revealed regardless of the response accuracy. Immediate retrieval continued until participants successfully recalled at least 60% (9 object-pairs) correctly.

In the morning session, participants were presented with the first object and were asked to click on the gray square representing the corresponding location of the object-pair (delayed retrieval). The location of the correct object-pair was not revealed to prevent additional encoding. Instead, the selected tile was highlighted by changing the color of the tile edges from white to cyan.

Delayed retrieval was repeated 3 weeks after the experimental night from home via video-call. Tiles were numbered so that participants verbally expressed their response to the experimenter who then clicked on the corresponding tile. This data is not presented.

All 30 object-pairs utilized in this study (**Supplementary Fig. 7)** were adopted from a previous study (Rasch et al., 2007).

Alterness task

Both in the evening and morning sessions, participants completed the alertness subtest of the Test of Attentional Performance (TAP) software (version 2.3.1; Zimmermann and Fimm, 2002). The alertness task assessed reaction times in two different conditions to evaluate both tonic and phasic alertness.

Tonic alertness was evaluated by measuring the reaction time (button press) in response to the appearance of a white cross on a black screen. Phasic alertness, on the other hand, was assessed by announcing the impending appearance of the white cross with a beep sound that was presented shortly before (with a random lag time).

The alertness task consisted of four blocks, with two blocks dedicated to assessing tonic alertness and the other two blocks focused on phasic alertness. Each block comprised 20 trials (tonic - phasic - phasic - tonic), resulting in a total of 80 trials across the entire task.

Finger sequence tapping task

Although the specific data from this test is not presented here due to the low number of participants, we will provide an explanation of the procedure for the sake of protocol completion.

In the evening session, participants engaged in a computerized finger sequence tapping task (adapted from Fattinger et al., 2017), and implemented using Psychopy (version 2020.1.3; Peirce et al., 2019). During the training trial, participants were instructed to type a simple sequence repeatedly for 30 seconds, aiming to complete as many repetitions as possible. Following the training trial, a 30-second rest period was given to prevent fatigue. Subsequently, participants completed 12 consecutive trials of typing the evening sequence. Each trial lasted 30 seconds and was followed by a 30-second rest period.

In the morning session, participants performed a new sequence for 12 consecutive trials, each lasting 30 seconds and separated by a 30-second rest period. Following the morning sequence, participants returned to type the evening sequence for 3 consecutive trials, with each trial lasting 30 seconds and separated by a 30-second rest period.

During the finger sequence tapping task, participants viewed the sequence on the screen, where the numbers 1, 2, 3, and 4 represented the index, middle, ring, and little finger of the right hand, respectively. As participants executed the sequence by tapping the corresponding keys, a black dot would appear below the current number on the screen to indicate that a response was recorded. However, no accuracy feedback was given during the task.

Upon completing a sequence, the screen was refreshed, displaying the same sequence, but with no black dots present. The training sequence consisted of the pattern 1-1-2-2-3-4. For the evening sequences, participants performed two different patterns: 2-4-1-3-1-2 and 2-1-3-1-4-2. In the morning session, two additional sequences were performed: 4-2-3-1-4-3 and 3-4-1-3-2-4.

Sleep hd-EEG recordings

During both experimental nights, hd-EEG data was recorded using an Electrical Geodesics Sensor Net for long-term monitoring (128 channels, Net Amps 400 series, Electrical Geodesics Inc., EGI, Eugene, OR) and acquired using EGI Net Station version 5.4. Electrooculographic (EOG) and submental electromyographic (EMG) signals were utilized for manual sleep scoring. To ensure optimal recording conditions, two additional electrodes (gold, Grass Technologies, West Warwick, RI) were attached to the earlobes and served as alternative references if necessary.

Electrocardiogram (ECG) electrodes (oval solid gel, Skintact, Innsbruck, AT) were positioned two fingers below the right clavicle and two fingers below the lowest left rib. After proper adjustment of the net to the vertex and mastoids, the skin underneath each electrode was prepared, and an electrolyte gel (ECI Electro-Gel, Electro-Cap International, Inc., Eaton, OH) was applied to ensure high conductance and maintain signal quality throughout the night. The impedance of the EEG electrodes was initially kept below 50 kΩ (5 kΩ for gold electrodes) at the start of the recording and rechecked in the morning. During recording, all channels were referenced to Cz and sampled at a rate of 500 Hz. The ECG was recorded using a bipolar reference configuration.

Subsequently, the EEG data was exported using EGI Net Station version 5.4, applying a specific 0.1 Hz high-pass filter to remove slow drifts and voltage jumps while ensuring the preservation of relevant frequency information.

Auditory stimulation

For real-time slow-wave detection and phase-locked auditory stimulation, a configurable mobile EEG system (referenced as MHSL-SleepBand in Ferster et al., 2019) was utilized. Stimulation triggers from the MHSL-SleepBand were sent as digital input to the EGI amplifier, allowing their integration into the hd-EEG signal.

Regarding the placement of electrodes for the MHSL-SleepBand, a gold electrode from Grass Technologies (West Warwick, RI) was positioned adjacent to C3, located between electrodes 29, 30, and 36 of the hd-EEG net, enabling real-time monitoring of EEG activity. Two additional gold electrodes were attached to the mastoids, serving as the ground (ipsilateral to the detection electrode) and the reference (contralateral to the detection electrode).

For the delivery of auditory stimuli, participants had on-ear headphones (sleepPhones, AcousticSheep LLC, Peninsula Drive, Pennsylvania) securely taped to their ears.

Auditory stimuli were presented at 50 dB. The loudness was verified using a sound level meter (UNI-T UT352 Type 2, Uni-Trend Technology EU GmbH, Augsburg, Germany). The measurement was taken with the

sound level meter placed directly against the headphones. Based on subjective perception, stimuli delivered via headphones were clearly audible.

A comprehensive description of the MHSL-SleepBand algorithm has been published previously (Ferster et al., 2019). In summary, the algorithm utilized three parallel binary classifiers:

1. *Sleep detection classifier:* This classifier continuously assessed increased SWA, reduced beta EEG activity, as well as the ratio of the two from the past 80 s of EEG to detect specific sleep stages, namely N2+N3 sleep. Sleep detection was satisfied when the predefined power thresholds were met.
2. *SWA classifier:* The SWA classifier continuously evaluated the SWA in the past 4 s of EEG signal. It aimed to detect as many slow waves as possible. When a predefined power threshold was met, SWA detection was satisfied.
3. *Phase detection classifier:* This classifier employed a phase-locked loop (PLL) architecture to estimate the phase of the input EEG signal. Its purpose was to identify the occurrence of 1 Hz waves and present auditory stimuli shortly before the negative peak of these slow waves.

When all three conditions were satisfied, an auditory stimulus in the form of a 50 ms tone of 1/f pink noise was delivered through headphones. The applied thresholds were optimized for the specific age group and electrode location by conducting simulations to evaluate algorithm performance based on previously collected data.

During the stimulation nights, auditory stimuli were presented during 16 second ON windows. These windows provided the opportunity for the delivery of auditory stimulation. In contrast, 8 second OFF windows were implemented to withhold auditory stimulation. In the SHAM night, the same timing flags for stimulation were recorded alongside the EEG data, but no actual auditory stimuli were presented.

Stimulation was applied throughout the entire night, starting after the detection of 10 minutes of stable NREM sleep. This ensured that auditory stimuli were administered during the targeted sleep stages of interest.

EEG preprocessing & sleep scoring

All EEG processing steps and analyses were performed in Matlab (R2017b, R2021b, R2022a, R2022b & R2023a) The Math-Works, Inc., Natick, Massachusetts) and EEGLAB (version 2021.1; Delorme and Makeig, 2004). Sleep scoring was performed using a software obtained from the Institute of Pharmacology and Toxicology of the University of Zurich, Switzerland.

Filters & down-sampling

The EEG data underwent several processing steps (**Supplementary Fig. 4)**. First, the EEG data was subjected to a low-pass filter with a cut-off of −6 dB at 39.86 Hz (filter order: 92 at a sampling rate of 500 Hz). Subsequently, the data was down-sampled to a sampling rate of 125 Hz and high-pass filtered with a cut-off of −6 dB at 0.37 Hz (filter order: 1494 at 125 Hz).

In recordings with strong sweat artifacts, as well as all corresponding recorded nights of the same participant, the EEG data was subjected to a stronger high-pass filter to ensure accurate sleep scoring. The high-pass filter had a cut-off of −6 dB at 0.75 Hz (filter order: 1246 at 125 Hz).

All filters, including those mentioned earlier and any subsequent filters, were Kaiser-window based FIR filters and were applied in a one-way manner with zero-phase shift, ensuring that filtering did not introduce any phase distortion. The filter order (in samples) is directly related to the sampling rate of the EEG, meaning that doubling the sampling rate would require doubling the filter order as well.

Sleep scoring

Sleep stages were manually scored in 20-second epochs by one sleep expert and verified by another sleep expert using EEG, EOG, and EMG signals. The scoring was conducted according to standard criteria (Berry et al., 2017), considering five vigilance stages: wake, N1, N2, N3, and REM sleep. Both scorers were blinded to the experimental condition and unaware of which night belonged to each participant. However, they were aware which nights belonged to the same participant.

For sleep scoring, the EEG data was referenced to the contralateral mastoid and down-sampled to 128 instead of 125 Hz to match the requirements of the scoring software.

The EOG data was high-pass filtered with a cut-off of −6 dB at 0.13 Hz (filter order: 1594 at 128 Hz) to preserve slow-rolling eye movements. The EMG data was low-pass filtered with a cut-off of −6 dB at 96.01 Hz (filter order: 230 at 500 Hz), notch filtered at 47.49 Hz (filter order: 368 at 500 Hz), down-sampled to 128 Hz, and high-pass filtered with a cut-off of −6 dB at 14.01 Hz (filter order: 64 at 128 Hz).

Artifact removal

During the manual sleep scoring process, any epoch containing artifacts in the channels visible during sleep scoring were excluded from further analyses. Afterward, 20-second epochs from 126 EEG channels (excluding the 2 submental EMG channels) were semi-automatically assessed using a custom graphical user interface (GUI) designed specifically for sleep hd-EEG data (Leach et al., 2023). In short, the raw EEG signal, as well as the distribution and topography of four sleep quality markers, were examined to detect artifactual NREM (N1+N2+N3) epochs. If more than two neighboring channels exhibited artifacts, the respective epoch was considered artifactual and removed. All remaining epochs were retained for subsequent EEG preprocessing steps.

Epoch-wise interpolation

Any channels marked with artifacts were subjected to interpolation in the affected epochs specifically using the *interpEPO()* function (Leach et al., 2023). As stated previously, only epochs in which no more than two neighboring channels contained artifacts were considered for interpolation.

Re-referencing

Unless specified otherwise, the EEG data was referenced to the mean of all 110 channels located above the ear (**Supplementary Fig. 8)**.

Analysis of sleep EEG

All subsequent analyses were performed exclusively on artifact-free NREM (N2+N3) epochs or ON|OFF windows. Functions for circular outcome measures (e.g., mean phase) were used from the toolbox for circular statistics (Berens, 2009). The mean of all channels and the channel average refer to the mean of the 110 channel above the ear if not stated otherwise.

Auditory-evoked potential (AEP)

The EEG data, referenced to the linked mastoids, was aligned to the first stimulus within ON windows and a short time-window (−0.4 – 3 s) was extracted. To compute the event-related potential (ERP), the EEG data within the selected time-windows was averaged across ON windows for a given channel and sample point. The AEP is the difference in ERP waveforms between conditions, thereby subtracting the underlying phase-locked slow wave (ERP in SHAM) from the AEP that is convoluted with the phase-locked slow wave (ERP in STIM).

Topography of N550

For each night, the latency of the N550 component was determined individually. This was done by identifying the latency of minimum value in the ERP waveform within a specific time-window (0.35 – 0.7 s) following the presentation of the first stimulus. The ERP consisted of the average signal from channels within a predefined frontal ROI.

Once the latency of the minimum value was identified, the corresponding amplitude at that latency was extracted in all channels. This amplitude represented the amplitude of the N550 component in a given channel.

Time-frequency analyses

Time-frequency analyses were performed using Morlet wavelets with 3 cycles at the lowest (0.5 Hz) to 12 cycles at the highest frequency (25 Hz), resulting in event-related spectral power (ERSP) and inter-trial coherence (ITC) values for 60 linearly spaced frequencies at 54 time points.

The average referenced EEG data was aligned to the onset of the first stimulus within an ON window. For a given ON window, EEG data within a short time-window (−3.56 – 5.88 s) was used as input for EEGLAB's *newtimef()* function (channel-wise). The resulting ERSP ranged between −213.16 and 2541.17 ms. They were subsequently normalized by dividing them by the average ERSP of the entire time-window (frequency-wise). The average ERSP over ON windows was calculated and stored for further analysis.

Cross-frequency coupling

Cross-frequency coupling of slow-waves and sleep spindles within 2 seconds following the onset of the first stimulus within an ON window was assessed using the *Modulation Index* (MI) (Tort et al., 2008), reviewed in Hülsemann et al. (2019).

Power- and phase-providing signal

To assess cross-frequency coupling, power and phase values were extracted using EEGLAB's *newtimef()* function. Morlet wavelets with 3 cycles at the lowest (0.5 Hz) and 5 cycles at the highest frequency (20 Hz) were employed. This choice of cycle numbers optimizes the temporal resolution required for accurate association of power values with specific phase bins, albeit at the expense of frequency precision.

EEG data within a short time-window (−3.344 – 5.344 s) was used as input for the computation of power and phase values (channel-wise). The resulting power and phase values were computed for 40 linearly spaced frequencies at 250 time points from 3.082 to 2004.92 ms post-stimulus. The values were not baseline corrected, as the final MI will be z-standardized.

Cross-frequency coupling was computed for different frequencies. The phase-providing signal comprised low frequencies in the slow-wave range (0.5 – 4 Hz in steps of 0.5 Hz) while the power-providing signal encompassed of higher frequencies in the sigma band (11 – 16 Hz in steps of 1 Hz). The MI was computed for all frequency pairs.

Modulation Index (MI)

To compute the MI, the power-providing signal in the sigma range was matched to the phase-providing signal in the slow-wave range. Phase estimates were grouped within conventional 18 bins of 20° each, representing a full circle. For each phase bin, the average power was computed, and subsequently, the empirical MI was calculated (channel-wise).

Z-standardized MI

To address potential confounding effects of power differences between STIM and SHAM nights on the MI, the empirical MI values were z-standardized. This procedure involves shuffling the power time-series 200 times while preserving the phase values (Cox et al., 2014; Kruglikova et al., 2020), thereby removing any systematic relationship between the two. The resulting distribution of MI values represents the null hypothesis of no phase-amplitude coupling. The empirical MI is then expressed in relation to this null distribution by calculating the z-score, indicating how many standard deviations the coupling estimate deviates from the average coupling estimate expected under the assumption of no coupling. The z-standardized MI (zMI) is independent of power differences between conditions, allowing for a more reliable comparison of cross-frequency coupling effects.

Power spectral density (PSD)

For each night, PSD values were calculated from average referenced EEG data. The PSD was computed using Matlab's *pwelch()* function (Welch method with 4-second Hanning windows, 50% overlap, and a frequency resolution of 0.25 Hz).

To compute overnight PSD values, EEG data within artifact-free N2, N3, or NREM (N2+N3) epochs were utilized. This resulted in separate overnight PSD values for N2 epochs, N3 epochs, and combined NREM epochs (N2+N3). Each epoch was divided into nine overlapping 4-second windows.

For PSD within ON|OFF windows, ON windows were divided into smaller segments (ON1, ON2, OFF), each with a duration of 8 seconds. Each segment was divided into three overlapping 4-second windows. Only ON|OFF windows that were entirely located within artifact-free NREM epochs were included in the analysis.

Overnight SWA

First, PSD values were averaged over epochs, separately for each frequency and channel (**Supplementary Fig. 2C**). For the computation of SWA, the lower boundary for SWA was set at 1 Hz due to the presence of sweat artifacts in some recordings. To obtain overnight SWA, averaged PSD values within the frequencies of interest (1 – 4.5 Hz) were summed and multiplied by the frequency resolution (0.25 Hz), separately for each channel (**Supplementary Fig. 2A**).

SWA within ON|OFF windows

For SWA within ON|OFF windows, PSD values were averaged over specific 8-second segments that corresponded to each ON|OFF window. ON|OFF windows were divided into three subsets based on the number of stimuli within the first 6 seconds of ON windows. These subsets corresponded to windows with few (1 – 2), medium (3 – 4), or many (5 – 8) stimuli, resulting in nine different window types (ON1, ON2, and OFF windows with either few, medium, or many stimuli).

For each window type, PSD values were averaged over windows, separately for each frequency and channel. SWA was calculated as described for overnight SWA. Percentage change between conditions was computed by taking the difference in SWA (STIM−SHAM) and dividing it by the SWA levels in SHAM (channel-wise).

Relative PSD within ON|OFF windows

Relative PSD values describe a redistribution (a shift) of PSD values within ON|OFF windows. To obtain relative PSD values, PSD values were divided by the channel average PSD of the entire ON|OFF window, separately for each frequency, window, and channel. For each of the nine window types, the mean of all channels and windows was computed to obtain average relative PSD values.

Phase estimation of auditory stimuli

To estimate the phase precision of presented stimuli (**Supplementary Fig. 1C**), the EEG data underwent filtering within the slow-wave range. For that, the EEG data was subjected to a low-pass filter with a cut-off of −6 dB at 5.00 Hz (filter order = 904 at 500 Hz), down-sampled to 125 Hz, and high-pass filtered with a cut-off of −6 dB at 0.37 Hz (filter order = 1494 at 125 Hz).

The EEG data was referenced to the linked mastoids and the first and last 14.940 samples (10 times the filter order) were set to zero. This step was performed to mitigate edge artifacts that could distort the Hilbert transform. Phase values were extracted by applying the *hilbert()* function to the EEG data of each channel. Phase values corresponding to the times of stimulation within artifact-free NREM (N2+N3) epochs were extracted and stored for further analysis.

Phase bins

For each participant, phase values were clustered into one of ten 30° bins (**Supplementary Fig. 1A**). This binning process involved using the mean phase value of channels 29, 30, and 36 (which are around the target electrode) with the help of the *circ_mean()* function. The percentage of values falling within each specific phase bin was then calculated.

Phase variance

The circular standard deviation of phase values was computed using the *circ_std()* function of the circular statistics toolbox, separately for each channel (**Supplementary Fig. 1B**).

Analysis of behavioral tasks

All behavioral data were analyzed in R (4.2.1) and RStudio (2022.07.1). Due to non-compliance with task instructions, one participant was excluded from the behavioral analyses. As a result, there were 13 complete datasets available for the analysis of the word-pair and alertness task, and 12 complete datasets for the object-location task.

Analysis of memory tasks

The number of correctly recalled word-pairs (object-pairs) in the evening and morning were used to assess overnight consolidation. The measure of overnight consolidation was computed as the difference in the number of correctly recalled items from morning to evening. Additionally, the number of correctly recalled word-pairs from the new list served as a measure of encoding capabilities the next morning.

In case participants required several trials to accomplish the 60% criterion, the number of correctly recalled items comprised the total number of correctly recalled items across trials.

Analysis of alertness task

Reaction times (RT, in ms) were averaged across trials within each block. For both phasic and tonic alertness, the average RTs were computed across blocks, along with their standard deviation. These measures provide an indication of alertness and sensitivity to sleep pressure (Doran et al., 2001; Gunzelmann et al., 2009). Overnight performance change was assessed by calculating the difference in average RT and the standard deviation of RT from morning to evening.

Correlations

Spearman's rank correlation was used to examine the relationship between the improvement in overnight memory consolidation of the associated word-pair task (STIM−SHAM) and the changes in the EEG induced by stimulation (STIM−SHAM; channel-wise). Specifically, correlations were performed on zMI values of all frequency combinations, and on ERSP values at all frequencies and time points.

Statistics

Statistics for EEG data and correlations were performed in MATLAB (R2022a, R2022b, R2023a, The Math-Works, Inc., Natick, Massachusetts). Statistics for behavioral data were performed in R (4.2.1) and RStudio (2022.07.1).

Topographical comparisons

For topographical comparisons between conditions (STIM−SHAM) of SWA, cross-frequency coupling, and the amplitude of the N550 component, paired Student's t-tests (α = .05, two-tailed) were performed (channel-wise). For topographical correlations between two variables, Spearman's rank correlation coefficients were computed (α = .05, two-tailed). To account for multiple comparisons, non-parametric cluster-based statistical mapping was applied (Nichols and Holmes, 2002).

Time-frequency comparisons

ERSP comparisons between conditions (STIM−SHAM) were examined using paired Student's t-tests (α = .001, two-tailed; pixel-wise). To account for multiple comparisons, non-parametric cluster-based statistical mapping was applied.

Non-parametric cluster-based statistical mapping

In short, the condition label (STIM or SHAM) was pseudo-randomly permuted across participants, so that participants pseudo-randomly switched conditions. The data was permuted 5000 times. The number of permutations is restricted by the number of participants ($2^N - 1$). Each permutation resulted in mutually exclusive condition labels. Paired Student's t-tests were performed in each permutation and the maximum cluster size of significant neighboring electrodes (or pixels) was computed, separately for positive and negative t-values. This resulted in two distributions of cluster sizes, one for positive and one for negative t-values, with as many values as permutations performed.

For topographical comparisons, the 97.5th percentile in each distribution, for the ERSP, the 99.9th percentile in each distribution was defined as the critical cluster size threshold, respectively. When the original data showed a cluster of significant electrodes (or pixels) equal or larger than the critical cluster size threshold, this cluster of electrodes (or pixels) was considered significant. Multiple clusters could co-exist.

AEP comparisons

AEP comparisons between conditions (STIM−SHAM) were performed at each sample point using paired Student's t-tests (α = .05, two-tailed; sample-wise). False discovery rate correction (Benjamini and Hochberg, 1995) was applied to account for multiple comparisons.

Behavioral comparisons

Comparisons of all behavioral measures between conditions (STIM−SHAM) were performed using paired Student's t-tests (α = .05, two-tailed).

Data availability

The raw EEG data, basic demographic information, responses to behavioral tests, actigraphy data, and sleep scoring files, fully anonymized, will be made accessible after an embargo period through a dedicated online repository for research data sharing.

References

Abel, T., Havekes, R., Saletin, J. M., and Walker, M. P. (2013). Sleep, plasticity and memory from molecules to whole-brain networks. *Current biology*, 23(17):R774–R788.

Alvarez, P. and Squire, L. R. (1994). Memory consolidation and the medial temporal lobe: a simple network model. *Proceedings of the national academy of sciences*, 91(15):7041–7045.

Amzica, F. and Steriade, M. (1997). The k-complex: its slow (< 1-hz) rhythmicity and relation to delta waves. *Neurology*, 49(4):952–959.

Baena, D., Fang, Z., Gibbings, A., Smith, D., Ray, L., Doyon, J., Owen, A. M., and Fogel, S. (2023). Functional differences in cerebral activation between slow wave-coupled and uncoupled sleep spindles. *Frontiers in Neuroscience*, 16:2334.

Bastien, C. and Campbell, K. (1992). The evoked k-complex: all-or-none phenomenon? *Sleep*, 15(3):236–245.

Benjamini, Y. and Hochberg, Y. (1995). Controlling the false discovery rate: a practical and powerful approach to multiple testing. *Journal of the Royal statistical society: series B (Methodological)*, 57(1):289–300.

Berens, P. (2009). Circstat: a matlab toolbox for circular statistics. *Journal of statistical software*, 31:1–21.

Bernardi, G., Siclari, F., Handjaras, G., Riedner, B. A., and Tononi, G. (2018). Local and widespread slow waves in stable nrem sleep: evidence for distinct regulation mechanisms. *Frontiers in human neuroscience*, 12:248.

Berry, R. B., Brooks, R., Gamaldo, C., Harding, S. M., Lloyd, R. M., Quan, S. F., Troester, M. T., and Vaughn, B. V. (2017). Aasm scoring manual updates for 2017 (version 2.4).

Colrain, I. M. (2005). The k-complex: a 7-decade history. *Sleep*, 28(2):255–273.

Cote, K. A., De Lugt, D. R., Langley, S. D., and Campbell, K. B. (1999). Scalp topography of the auditory evoked k-complex in stage 2 and slow wave sleep. *Journal of Sleep Research*, 8(4):263–272.

Cox, R., Rüber, T., Staresina, B. P., and Fell, J. (2019). Heterogeneous profiles of coupled sleep oscillations in human hippocampus. *NeuroImage*, 202:116178.

Cox, R., van Driel, J., de Boer, M., and Talamini, L. M. (2014). Slow oscillations during sleep coordinate interregional communication in cortical networks. *Journal of Neuroscience*, 34(50):16890–16901.

Crunelli, V., Lőrincz, M. L., Errington, A. C., and Hughes, S. W. (2012). Activity of cortical and thalamic neurons during the slow (< 1 hz) rhythm in the mouse in vivo. *Pflügers Archiv-European Journal of Physiology*, 463(1):73–88.

Dang-Vu, T. T., Schabus, M., Desseilles, M., Albouy, G., Boly, M., Darsaud, A., Gais, S., Rauchs, G., Sterpenich, V., Vandewalle, G., et al. (2008). Spontaneous neural activity during human slow wave sleep. *Proceedings of the National Academy of Sciences*, 105(39):15160–15165.

Davis, H., Davis, P. A., Loomis, A. L., Harvey, E. N., and Hobart, G. (1939). Electrical reactions of the human brain to auditory stimulation during sleep. *Journal of Neurophysiology*, 2(6):500–514.

De Gennaro, L., Gorgoni, M., Reda, F., Lauri, G., Truglia, I., Cordone, S., Scarpelli, S., Mangiaruga, A., D'atri, A., Lacidogna, G., et al. (2017). The fall of sleep k-complex in alzheimer disease. *Scientific reports*, 7(1):1–9.

Delorme, A. and Makeig, S. (2004). Eeglab: an open source toolbox for analysis of single-trial eeg dynamics including independent component analysis. *Journal of neuroscience methods*, 134(1):9–21.

Diekelmann, S. and Born, J. (2010). The memory function of sleep. *Nature Reviews Neuroscience*, 11(2):114–126.

Doran, S. M., Van Dongen, H. P., and Dinges, D. F. (2001). Sustained attention performance during sleep deprivation: evidence of state instability. *Archives italiennes de biologie*, 139(3):253–267.

Ego-Stengel, V. and Wilson, M. A. (2010). Disruption of ripple-associated hippocampal activity during rest impairs spatial learning in the rat. *Hippocampus*, 20(1):1–10.

Fattinger, S., de Beukelaar, T. T., Ruddy, K. L., Volk, C., Heyse, N. C., Herbst, J. A., Hahnloser, R. H., Wenderoth, N., and Huber, R. (2017). Deep sleep maintains learning efficiency of the human brain. *Nature communications*, 8(1):1–14.

Ferino, F., Thierry, A., and Glowinski, J. (1987). Anatomical and electrophysiological evidence for a direct projection from ammon's horn to the medial prefrontal cortex in the rat. *Experimental brain research*, 65(2):421–426.

Fernandez, L. M. and Lüthi, A. (2020). Sleep spindles: mechanisms and functions. *Physiological reviews*, 100(2):805–868.

Ferster, M. L., Lustenberger, C., and Karlen, W. (2019). Configurable mobile system for autonomous high-quality sleep monitoring and closed-loop acoustic stimulation. *IEEE Sensors Letters*, 3(5):1–4.

Fletcher, P. and Dolan, R. J. (1999). Right prefrontal cortex responds to item familiarity during a memory encoding task. *Memory*, 7(5-6):703–715.

Genzel, L., Kroes, M. C., Dresler, M., and Battaglia, F. P. (2014). Light sleep versus slow wave sleep in memory consolidation: a question of global versus local processes? *Trends in neurosciences*, 37(1):10–19.

Geva-Sagiv, M., Mankin, E. A., Eliashiv, D., Epstein, S., Cherry, N., Kalender, G., Tchemodanov, N., Nir, Y., and Fried, I. (2023). Augmenting hippocampal–prefrontal neuronal synchrony during sleep enhances memory consolidation in humans. *Nature Neuroscience*, pages 1–11.

González-Rueda, A., Pedrosa, V., Feord, R. C., Clopath, C., and Paulsen, O. (2018). Activity-dependent downscaling of subthreshold synaptic inputs during slow-wave-sleep-like activity in vivo. *Neuron*, 97(6):1244–1252.

Gora, J., Colrain, I. M., and Trinder, J. (2001). The investigation of k-complex and vertex sharp wave activity in response to mid-inspiratory occlusions and complete obstructions to breathing during nrem sleep. *Sleep*, 24(1):81–89.

Gunzelmann, G., Gross, J. B., Gluck, K. A., and Dinges, D. F. (2009). Sleep deprivation and sustained attention performance: Integrating mathematical and cognitive modeling. *Cognitive science*, 33(5):880–910.

Hager, W. and Hasselhorn, M. (1994). Handbuch deutschsprachiger wortnormen hogrefe. *Verlag für Psychologie Göttingen, Bern, Toronto, Seattle*.

Hahn, M. A., Heib, D., Schabus, M., Hoedlmoser, K., and Helfrich, R. F. (2020). Slow oscillation-spindle coupling predicts enhanced memory formation from childhood to adolescence. *Elife*, 9:e53730.

Halasz, P. (1993). Arousals without awakening—dynamic aspect of sleep. *Physiology & behavior*, 54(4):795–802.

Halász, P. (2005). K-complex, a reactive eeg graphoelement of nrem sleep: an old chap in a new garment. *Sleep medicine reviews*, 9(5):391–412.

Harrington, M. O. and Cairney, S. A. (2021). Sounding it out: Auditory stimulation and overnight memory processing. *Current Sleep Medicine Reports*, 7(3):112–119.

Helfrich, R. F., Mander, B. A., Jagust, W. J., Knight, R. T., and Walker, M. P. (2018). Old brains come uncoupled in sleep: slow wave-spindle synchrony, brain atrophy, and forgetting. *Neuron*, 97(1):221–230.

Hülsemann, M. J., Naumann, E., and Rasch, B. (2019). Quantification of phase-amplitude coupling in neuronal oscillations: comparison of phase-locking value, mean vector length, modulation index, and generalized-linear-modeling-cross-frequency-coupling. *Frontiers in neuroscience*, 13:573.

Huwiler, S., Dominguez, M. C., Huwyler, S., Kiener, L., Stich, F., Sala, R., Aziri, F., Trippel, A., Schmied, C., Huber, R., et al. (2022). Effects of auditory sleep modulation approaches on brain oscillatory and cardiovascular dynamics. *bioRxiv*.

Isomura, Y., Sirota, A., Özen, S., Montgomery, S., Mizuseki, K., Henze, D. A., and Buzsáki, G. (2006). Integration and segregation of activity in entorhinal-hippocampal subregions by neocortical slow oscillations. *Neuron*, 52(5):871–882.

Johnson, L. C. and Lubin, A. (1967). The orienting reflex during waking and sleeping. *Electroencephalography and clinical neurophysiology*, 22(1):11–21.

Klinzing, J. G., Niethard, N., and Born, J. (2019). Mechanisms of systems memory consolidation during sleep. *Nature neuroscience*, 22(10):1598–1610.

Krugliakova, E., Skorucak, J., Sousouri, G., Leach, S., Snipes, S., Ferster, M. L., Da Poian, G., Karlen, W., and Huber, R. (2022). Boosting recovery during sleep by means of auditory stimulation. *Frontiers in neuroscience*, 16.

Krugliakova, E., Volk, C., Jaramillo, V., Sousouri, G., and Huber, R. (2020). Changes in cross-frequency coupling following closed-loop auditory stimulation in non-rapid eye movement sleep. 10(1):1–12.

Kurella, B., Heitmann, A., Golz, M., and Dormann, U. (1992). The probability of eliciting k-complexes during sleep. *J Sleep Res*, 1(suppl 1):124.

Landwehr, R. (2007). Detection of activation phases and quantification of coupling in nrem sleep eeg by pointwise transinformation. *Sleep Medicine*, 8(1):65–72.

Latchoumane, C.-F. V., Ngo, H.-V. V., Born, J., and Shin, H.-S. (2017a). Thalamic spindles promote memory formation during sleep through triple phase-locking of cortical, thalamic, and hippocampal rhythms. *Neuron*, 95(2):424–435.

Latchoumane, C.-F. V., Ngo, H.-V. V., Born, J., and Shin, H.-S. (2017b). Thalamic spindles promote memory formation during sleep through triple phase-locking of cortical, thalamic, and hippocampal rhythms. *Neuron*, 95(2):424–435.

Laurino, M., Menicucci, D., Piarulli, A., Mastorci, F., Bedini, R., Allegrini, P., and Gemignani, A. (2014). Disentangling different functional roles of evoked k-complex components: mapping the sleeping brain while quenching sensory processing. *Neuroimage*, 86:433–445.

Leach, S., Sousouri, G., and Huber, R. (2023). 'high-density-sleepcleaner': An open-source, semi-automatic artifact removal routine tailored to high-density sleep eeg. *Journal of Neuroscience Methods*, 391:109849.

Leminen, M. M., Virkkala, J., Saure, E., Paajanen, T., Zee, P. C., Santostasi, G., Hublin, C., Müller, K., Porkka-Heiskanen, T., Huotilainen, M., et al. (2017). Enhanced memory consolidation via automatic sound stimulation during non-rem sleep. *Sleep*, 40(3).

Lewis, P. A. and Durrant, S. J. (2011). Overlapping memory replay during sleep builds cognitive schemata. *Trends in cognitive sciences*, 15(8):343–351.

Loomis, A. L., Harvey, E. N., and Hobart, G. (1935). Potential rhythms of the cerebral cortex during sleep. *Science*, 81(2111):597–598.

Lustenberger, C., Ferster, M. L., Huwiler, S., Brogli, L., Werth, E., Huber, R., and Karlen, W. (2022). Auditory deep sleep stimulation in older adults at home: a randomized crossover trial. *Communications Medicine*, 2(1):1–16.

Lüthi, A. (2014). Sleep spindles: where they come from, what they do. *The Neuroscientist*, 20(3):243–256.

Maingret, N., Girardeau, G., Todorova, R., Goutierre, M., and Zugaro, M. (2016). Hippocampo-cortical coupling mediates memory consolidation during sleep. *Nature neuroscience*, 19(7):959–964.

Marshall, L., Helgadóttir, H., Mölle, M., and Born, J. (2006). Boosting slow oscillations during sleep potentiates memory. *Nature*, 444(7119):610–613.

Mölle, M., Marshall, L., Gais, S., and Born, J. (2002). Grouping of spindle activity during slow oscillations in human non-rapid eye movement sleep. *Journal of Neuroscience*, 22(24):10941–10947.

Moreira, C. G., Baumann, C. R., Scandella, M., Nemirovsky, S. I., Leach, S., Huber, R., and Noain, D. (2021). Closed-loop auditory stimulation method to modulate sleep slow waves and motor learning performance in rats. *Elife*, 10:e68043.

Mottaghy, F., Shah, N., Krause, B., Schmidt, D., Halsband, U., Jäncke, L., and Müller-Gärtner, H.-W. (1999). Neuronal correlates of encoding and retrieval in episodic memory during a paired-word association learning task: a functional magnetic resonance imaging study. *Experimental Brain Research*, 128:332–342.

Navarrete, M., Osorio-Forero, A., Gómez, A., Henao, D., Le Van Quyen, M., and Valderrama, M. (2022). Response of sleep slow oscillations to acoustic stimulation is evidenced by distinctive synchronization processes. *bioRxiv*, pages 2022–05.

Neckelmann, D. and Ursin, R. (1993). Sleep stages and eeg power spectrum in relation to acoustical stimulus arousal threshold in the rat. *Sleep*, 16(5):467–477.

Ngo, H.-V., Fell, J., and Staresina, B. (2020). Sleep spindles mediate hippocampal-neocortical coupling during long-duration ripples. *elife*, 9:e57011.

Ngo, H.-V. V., Martinetz, T., Born, J., and Mölle, M. (2013a). Auditory closed-loop stimulation of the sleep slow oscillation enhances memory. *Neuron*, 78(3):545–553.

Ngo, H.-V. V., Martinetz, T., Born, J., and Mölle, M. (2013b). Auditory closed-loop stimulation of the sleep slow oscillation enhances memory. *Neuron*, 78(3):545–553.

Ngo, H.-V. V., Miedema, A., Faude, I., Martinetz, T., Mölle, M., and Born, J. (2015). Driving sleep slow oscillations by auditory closed-loop stimulation—a self-limiting process. *Journal of Neuroscience*, 35(17):6630–6638.

Nichols, T. E. and Holmes, A. P. (2002). Nonparametric permutation tests for functional neuroimaging: a primer with examples. *Human brain mapping*, 15(1):1–25.

Ong, J. L., Lo, J. C., Chee, N. I., Santostasi, G., Paller, K. A., Zee, P. C., and Chee, M. W. (2016). Effects of phase-locked acoustic stimulation during a nap on eeg spectra and declarative memory consolidation. *Sleep medicine*, 20:88–97.

Papalambros, N. A., Santostasi, G., Malkani, R. G., Braun, R., Weintraub, S., Paller, K. A., and Zee, P. C. (2017). Acoustic enhancement of sleep slow oscillations and concomitant memory improvement in older adults. *Frontiers in human neuroscience*, 11:109.

Papalambros, N. A., Weintraub, S., Chen, T., Grimaldi, D., Santostasi, G., Paller, K. A., Zee, P. C., and Malkani, R. G. (2019). Acoustic enhancement of sleep slow oscillations in mild cognitive impairment. *Annals of clinical and translational neurology*, 6(7):1191–1201.

Peirce, J., Gray, J. R., Simpson, S., MacAskill, M., Höchenberger, R., Sogo, H., Kastman, E., and Lindeløv, J. K. (2019). Psychopy2: Experiments in behavior made easy. *Behavior research methods*, 51(1):195–203.

Peyrache, A., Battaglia, F. P., and Destexhe, A. (2011). Inhibition recruitment in prefrontal cortex during sleep spindles and gating of hippocampal inputs. *Proceedings of the National Academy of Sciences*, 108(41):17207–17212.

Rasch, B. and Born, J. (2013). About sleep's role in memory. *Physiological reviews*.

Rasch, B., Büchel, C., Gais, S., and Born, J. (2007). Odor cues during slow-wave sleep prompt declarative memory consolidation. *Science*, 315(5817):1426–1429.

Roth, M., Shaw, J., and Green, J. (1956). The form, voltage distribution and physiological significance of the k-complex. *Electroencephalography and clinical neurophysiology*, 8(3):385–402.

Schreiner, S. J., Imbach, L. L., Werth, E., Poryazova, R., Baumann-Vogel, H., Valko, P. O., Murer, T., Noain, D., and Baumann, C. R. (2019). Slow-wave sleep and motor progression in parkinson disease. *Annals of neurology*, 85(5):765–770.

Siclari, F., Bernardi, G., Riedner, B. A., LaRocque, J. J., Benca, R. M., and Tononi, G. (2014). Two distinct synchronization processes in the transition to sleep: a high-density electroencephalographic study. *Sleep*, 37(10):1621–1637.

Sirota, A., Csicsvari, J., Buhl, D., and Buzsáki, G. (2003). Communication between neocortex and hippocampus during sleep in rodents. *Proceedings of the National Academy of Sciences*, 100(4):2065–2069.

Sousouri, G., Krugliakova, E., Skorucak, J., Leach, S., Snipes, S., Ferster, M. L., Da Poian, G., Karlen, W., and Huber, R. (2022). Neuromodulation by means of phase-locked auditory stimulation affects key marker of excitability and connectivity during sleep. *Sleep*, 45(1):zsab204.

Squire, L. R., Genzel, L., Wixted, J. T., and Morris, R. G. (2015). Memory consolidation. *Cold Spring Harbor perspectives in biology*, 7(8):a021766.

Staresina, B. P., Bergmann, T. O., Bonnefond, M., Van Der Meij, R., Jensen, O., Deuker, L., Elger, C. E., Axmacher, N., and Fell, J. (2015). Hierarchical nesting of slow oscillations, spindles and ripples in the human hippocampus during sleep. *Nature neuroscience*, 18(11):1679–1686.

Steriade, M., McCormick, D. A., and Sejnowski, T. J. (1993). Thalamocortical oscillations in the sleeping and aroused brain. *Science*, 262(5134):679–685.

Stern, J. M. (2005). *Atlas of EEG patterns*. Lippincott Williams & Wilkins.

Stickgold, R. (2005). Sleep-dependent memory consolidation. *Nature*, 437(7063):1272–1278.

Takehara-Nishiuchi, K. (2021). Neurobiology of systems memory consolidation. *European Journal of Neuroscience*, 54(8):6850–6863.

Teyler, T. J. and DiScenna, P. (1986). The hippocampal memory indexing theory. *Behavioral neuroscience*, 100(2):147.

Timofeev, I. and Chauvette, S. (2017). Sleep slow oscillation and plasticity. *Current opinion in neurobiology*, 44:116–126.

Tononi, G. and Cirelli, C. (2014). Sleep and the price of plasticity: from synaptic and cellular homeostasis to memory consolidation and integration. *Neuron*, 81(1):12–34.

Tort, A. B., Kramer, M. A., Thorn, C., Gibson, D. J., Kubota, Y., Graybiel, A. M., and Kopell, N. J. (2008). Dynamic cross-frequency couplings of local field potential oscillations in rat striatum and hippocampus during performance of a t-maze task. *Proceedings of the National Academy of Sciences*, 105(51):20517–20522.

Vyazovskiy, V. V., Olcese, U., Lazimy, Y. M., Faraguna, U., Esser, S. K., Williams, J. C., Cirelli, C., and Tononi, G. (2009). Cortical firing and sleep homeostasis. *Neuron*, 63(6):865–878.

Walker, M. P. (2005). A refined model of sleep and the time course of memory formation. *Behavioral and brain sciences*, 28(1):51–64.

Wierzynski, C. M., Lubenov, E. V., Gu, M., and Siapas, A. G. (2009). State-dependent spike-timing relationships between hippocampal and prefrontal circuits during sleep. *Neuron*, 61(4):587–596.

Wilhelm, I., Diekelmann, S., and Born, J. (2008). Sleep in children improves memory performance on declarative but not procedural tasks. *Learning & memory*, 15(5):373–377.

Zhang, Y. and Gruber, R. (2019). Focus: attention science: can slow-wave sleep enhancement improve memory? a review of current approaches and cognitive outcomes. *The Yale journal of biology and medicine*, 92(1):63.

Zielinski, M. R. and Krueger, J. M. (2011). Sleep and innate immunity. *Frontiers in bioscience (Scholar edition)*, 3:632.

Zimmermann, P. and Fimm, B. (2002). *Testbatterie zur Aufmerksamkeitsprüfung:(TAP), Version 1.7*. Psytest.